Simulation of head-first impact using cervical spine specimens, simulated neck muscles, and a Hybrid III ATD head

C. Van Toen[1], C. F. Jones[1], T. S. Nelson[1], J. Street[2] and P. A. Cripton[1]
[1] Injury Biomechanics Laboratory, Department of Mechanical Engineering, University of British Columbia; [2] Department of Orthopaedics, University of British Columbia

ABSTRACT

Neck muscles stiffen and stabilize the cervical spine; however, their influence during ex vivo axial impact experiments has previously only been examined for highly simplified musculature. The objective of this study was to create a model of head-first impact with simulation of several major neck muscles, using a Hybrid III ATD head and cadaver cervical spine to create compressive cervical spine injuries. Five osteoligamentous cervical spines (Occ-T2) were potted in dental stone at T1/2, mounted on a six-axis load cell and attached to a Hybrid III head at the occiput. Four bilateral muscles and three follower load cables were included. Fishing line was tied to vertebrae or to the adapter plate at the occiput and connected to springs to simulate muscle forces. Specimens were mounted to the carriage of a drop tower and dropped onto an impact platform overtop a uniaxial load cell while high speed video cameras captured the impacts. Injuries were diagnosed by a fellowship-trained spine surgeon (JS). Specimens were aligned to minimize eccentricity (anteroposterior distance between the occipital condyles and T1 vertebral body). Average segmental compression forces were 109 (SD 38) N at C0/1 and this increased inferiorly. Average peak head and lower neck axial loads were 6,893 (SD 791) N and 2,635 (SD 1096) N, respectively. Injuries included burst fractures, disc ruptures, and facet capsule ruptures. This pilot study showed that clinically relevant compression injuries in head-first impacts can be reproduced with simulation of muscle forces that allow detailed control of spinal posture. As we tied muscle simulating cables to the vertebrae, this was achieved without producing stress risers or damaging the structural integrity of the spinal column.

INTRODUCTION

Spinal cord injuries (SCI) are a significant health concern with an annual incidence of 13,000 in the United States (Dryden et al. 2003; NSCISC 2006) resulting in devastating consequences for victims and their families. Axial loading of the cervical spine leading to

SCI may result from any head-first impact and has been implicated as the prime mechanism leading to SCI in football and in motor vehicle accidents (Yoganandan et al. 1989; Torg et al. 2002). Although neck muscles stiffen and stabilize the cervical spine, their influence during *ex vivo* axial impact experiments has previously only been examined for highly simplified musculature and this was work in our lab (Saari et al. 2006). Experimental models of whiplash and stability have simulated the effect of muscle forces; however, the techniques used to attach these forces altered the structural integrity of the spinal column, as rods and/or screws were inserted into the vertebrae (Panjabi et al. 2001; Kettler et al. 2002). Since axial compression typically results in vertebral fractures, any stress risers in the bone, due to rods or screws, would be undesirable as they could cause non-physiologic fracture initiation. Deep and surface muscle activation during head-first impact has not been simulated in an experimental model. Such a model would be useful for incorporating the activation of muscles from *in vivo* studies and to validate computational models. The objective of this study was to create an experimental model of head-first impact with simulation of several major neck muscles, using a Hybrid III ATD head and cadaver cervical spine to create compressive cervical spine injuries.

METHODS

Five fresh human cervical spines (occiput to T2) were harvested, screened radiographically for bony abnormalities, loss of disc height, or other signs of abnormal degeneration, and frozen until use. The average age of the donors was 79 (SD 12) years and two donors were female.

The experimental apparatus was designed to simulate a head-first impact. Specimens were mounted in an inverted posture on the carriage of a custom drop tower. The carriage had a mass of 17 kg, which approximated the effective mass of the torso in a diving injury (Nightingale et al. 1996). Specimens were dropped from a height of 60 cm to achieve an impact velocity of approximately 3 m/s. The impact platform was covered with a padded, high friction surface. A uniaxial load cell was placed underneath the impact platform (Omega LC 402-5K). T1 and T2 were potted in a casting cup with dental stone which was attached to an aluminum plate and to a six-axis lower neck load cell (Denton 4366J), which was mounted to the carriage of the drop tower (Figure 1A). A portion of the occiput was attached to a 50th percentile Hybrid III ATD head using custom adapter plates and epoxy putty (Magic Bond, Devcon, Danvers MA).

The Advanced Muscle Force Replication (AMFR) system was developed to simulate the forces of four superficial bilateral muscles or groups of muscles: semispinalis capitis, sternocleidomastoid, hyoid (omohyoid, sternohyoid, and sternothyroid), and trapezius using high strength braided fishing line (Gorilla Tough, Berkely, Spirit Lake IA). Deep neck musculature was simulated with an anterior follower load and two lateral follower loads, which were guided at each vertebral level (C1-7) and around the casting cup using two pulleys (Figure 1A) to provide compression along the length of the spine. The fishing line muscle cables were fixed to the occiput adapter plate, to the occiput, and/or to the vertebrae (Figure 1A). To fix the AMFR cables on each vertebra without screws, hinged clamps and split rings were attached to vertebral harnesses: additional fishing line that was tied around foramina and into the spinal canal on each vertebra (C1-C7) (Figure 1B). Some AMFR cables passed through holes in the aluminum plate that located the inferior attachments of the muscles, which were based on published quantitative anatomical dissections (Chancey et al. 2003; Oi et al. 2004). Each cable was tied to a spring-screw assembly (compression spring stiffness 3.15 N/mm) such that turning a nut on the screw applied tension to the cable. The semispinalis capitis muscle was simulated using eight extension springs (1.19 N/mm) attached bilaterally to C4-7 and the occiput. Spring lengths were controlled with screws and nuts. Bilateral flexion limiting cables were tied between the occiput and C1 to avoid hyperflexion of the specimen, which would be prevented in a living subject by contact between the chin and chest (Panjabi et al. 2001).

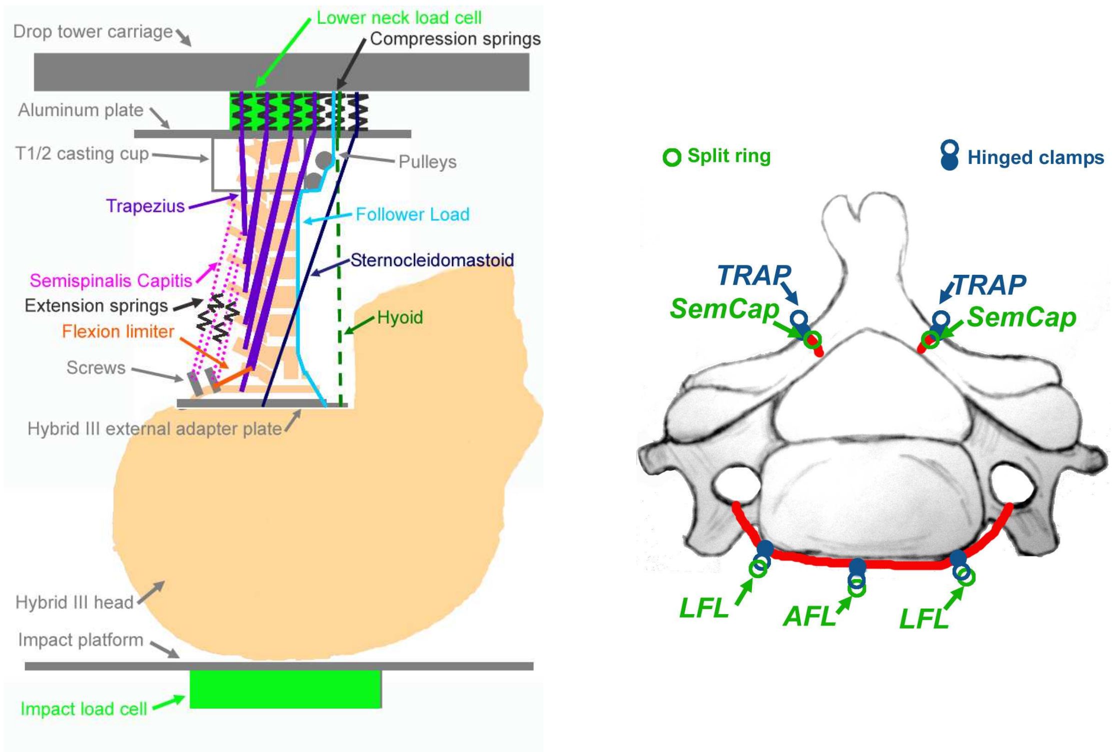

A B

Figure 1. (A) Schematic of the AMFR system (lateral view) with muscle cables and key components identified. (B) Superior view of a typical cervical vertebra showing the path of the vertebral harness: braided fishing line tied to the vertebra and used along with hinged clamps and split rings to provide non-destructive attachment points for muscle force cables. AMFR cables using each attachment point are listed (LFL: lateral follower load, AFL: anterior follower load, TRAP: trapezius, SemCap: semispinalis capitis).

The muscle forces were adjusted as necessary to vertically align the impact point on the head, the occipital condyles, and the center of the T1 vertebral body. Spring lengths were measured following specimen alignment and before drop tests. These were used to determine muscle forces and resultant segmental forces (the sum of the muscle forces acting through each segment, without taking into consideration the angles of the muscle lines of action or the posture of each segment). Impacts were captured with two high speed video cameras (Phantom V9, Vision Research, Wayne NJ) at 1000 frames per second. Load cell data were image-synchronized, sampled at 78 kHz and filtered to satisfy SAE standard J211b. Injuries were diagnosed by a spine surgeon (JS) using x-ray, CT, and post-test dissection.

RESULTS

By increasing the spring compression/extension in the muscle force and follower load cables, the cervical lordosis was removed from specimens and they were aligned with minimal lordosis or sagittal plane misalignment between the impact point on the head, the occipital condyles, and T1. With the AMFR system applied, the specimens felt qualitatively much more stiff, stable and human-like than did the osteoligamentous cervical spines without the AMFR system. The average total force in the muscle cables was 205.8 (SD 34.0) N. Average resultant segmental forces increased caudally: 109 (SD 38) N at C0/1, 117 (SD 36) N at C1/2, 128 (SD 31) N at C2/3, 139 (SD 26) N at C3/4, 155 (SD 22) N at C4/5, 172 (SD 24) N at C5/6, 181 (SD 25) N at C6/7 and 189 (SD 26) N at C7/T1.

Table 1: Peak forces at the impact platform and forces and moments at the lower neck load cell.

Specimen	Head Impact Force (N)	Lower Neck Force (N)			Lower Neck Moments (Nm)		
		Antero-posterior Shear	Lateral Shear	Axial	Lateral Bending	Flexion/ Extension	Axial Rotation
1220	7926	571	233	3835	32.7	112.0	7.0
1221	7442	473	143	2303	15.1	81.8	6.3
1222	6525	896	175	3756	21.5	101.3	7.6
1223	6650	337	128	1758	12.1	59.6	5.6
1224	5923	757	164	1525	9.5	104.3	7.5
Average	**6893**	**607**	**168**	**2635**	**18.2**	**91.8**	**6.8**
SD	**791**	**223**	**40**	**1096**	**9.3**	**21.2**	**0.9**

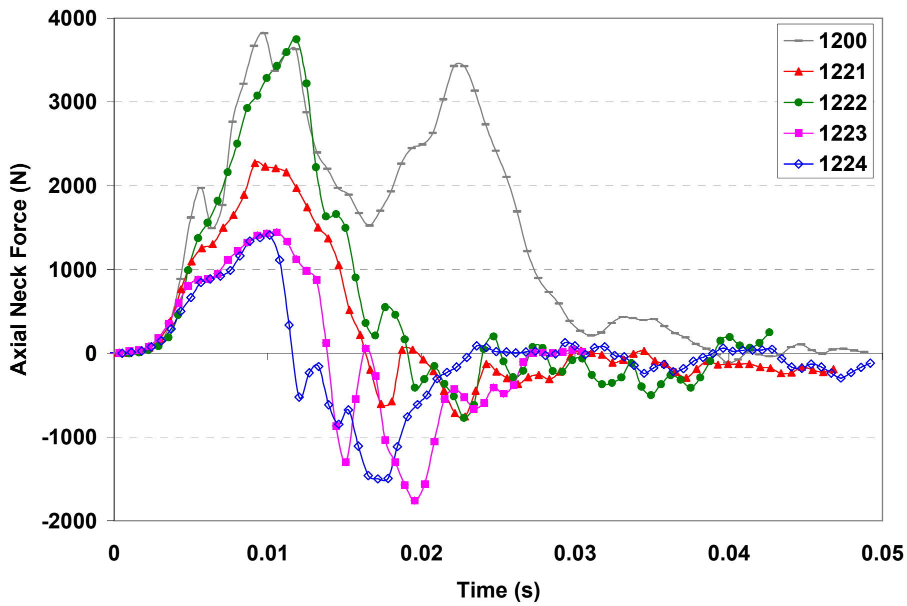

Figure 2: Lower neck axial force vs. time (specimen numbers are listed in the legend). Positive forces are compressive and negative forces are tensile.

Average peak impact and lower neck axial loads were 6,893 (SD 791) N and 2635 (SD 1096) N (Table 1). Peak lower neck axial forces generally occurred while the Hybrid III head was moving upward during rebound and the carriage was moving downward. While the lower neck axial force of specimen 1220 exhibited two peaks greater than 3000 N, those of the other specimens exhibited one peak in compression followed by axial tension as the head moved cranially and into extension during rebound (Figure 2).

The injuries produced included upper cervical spine compression fractures: burst and Jefferson type III fractures of the atlas, and Hangman and dens fractures of the axis. The C7/T1 segment of specimens 1221-1224 exhibited ligamentum flavum rupture with facet capsule rupture, endplate fracture, vertebral body fracture, anterior longitudinal ligament rupture and/or interspinous ligament rupture at this level. These specimens also exhibited extension-type injuries in the mid-cervical levels (C3-6), such as open anterior disc spaces, and spinous process fractures. Injury details are provided in Appendix A.

DISCUSSION

Cervical spine and head kinetics are central to understanding injury mechanisms during simulated head-first impact and may play a key role in developing injury prevention devices, and in linking clinical diagnoses and treatment strategies. Our experimental model of compressive spine injuries with simulation of muscle forces may allow for simulation of neck muscle activation from *in vivo* studies to be incorporated in our experiments and the present results could be used to validate computational models.

The peak forces and injuries produced in this experimental model are similar to those previously reported without simulation of neck muscles (Nightingale et al. 1996). While specimen 1220 exhibited primarily compression-type injuries, the other specimens exhibited compression-extension injuries in the mid-cervical levels and compression-flexion injuries at C7/T1. This difference may be partly due to variations in the alignment of the occiput on the adapter plate, which may have caused specimens 1221-1224 to be loaded in a slightly extended posture. This was noted during application of the muscle forces. The injuries at C7/T1 may be associated with boundary constraints as rotation of the molded T1 vertebrae with respect to the impact carriage was not allowed.

The AMFR system allowed posture to be controlled directly with simulated muscle forces applied at each vertebral level, rather than indirectly through head positioning, which was used in previous models (Pintar et al. 1990; Nightingale et al. 1996; Saari et al. 2006). The muscle cables acted to stabilize the spine during the initial phases of head impact and the related increase in neck loading. Simulation of muscle forces was achieved without compromising the structural integrity of the spine, which we feel is essential to avoid stress concentrations. Limitations of the AMFR system include the considerable amount of time required to attach the muscle cables and technical challenges in aligning the occiput on the adapter plate. The model assumes muscles behave in a linear elastic manner and have point attachments, whereas they are known to be viscoelastic and have distributed tendon insertions. To our knowledge, no previous study has examined segmental forces in the cervical spine in an inverted posture or in a startled individual, as may be the case prior to a head impact. However, the segmental forces generated by the AMFR system (132-190 at C4-5) are within the range of compression forces previously reported for a variety of postures and muscle activations (53-558 N) (Hattori et al. 1981; Moroney et al. 1988).

CONCLUSIONS

This pilot study showed that clinically relevant compression injuries in head-first impacts can be reproduced with a cadaver spine, Hybrid III head, and simulated muscle forces through the use of the AMFR system. This model advances *ex vivo* testing as it permits simulation of neck muscle forces without reduction of the structural integrity of the spinal column.

ACKNOWLEDGEMENTS

The authors would like to acknowledge the Natural Sciences and Engineering Research Council of Canada (NSERC) for funding this work, the Canada Foundation of Innovation and British Columbia Knowledge Development Fund for funding equipment purchases and Denton ATD for their assistance.

REFERENCES

Chancey, V. C., R. W. Nightingale, et al. (2003). "Improved estimation of human neck tensile tolerance: reducing the range of reported tolerance using anthropometrically correct muscles and optimized physiologic initial conditions." Stapp Car Crash J. **47**: 135-53.

Dryden, D. M., L. D. Saunders, et al. (2003). "The epidemiology of traumatic spinal cord injury in Alberta, Canada." Can J Neurol Sci. **30**(2): 113-21.

Hattori, S., H. Oda, et al. (1981). "Cervical intradiscal pressure in movements and traction of the cervical spine." Zeitschrift fur Orthopadie **119**: 568-569.

Kettler, A., E. Hartwig, et al. (2002). "Mechanically simulated muscle forces strongly stabilize intact and injured upper cervical spine specimens." J Biomech. **35**(3): 339-46.

Moroney, S. P., A. B. Schultz, et al. (1988). "Analysis and measurement of neck loads." Journal of Orthopaedic Research **6**: 713-720.

Nightingale, R. W., J. H. McElhaney, et al. (1996). "Dynamic response of the head and cervical spine to axial impact loading." Journal of Biomechanics **29**(3): 307-318.

NSCISC (2006). Spinal Cord Injury Facts and Figures at a Glance. National Spinal Cord Injury Statistical Center. Birmingham, Alabama, University of Alabama.

Oi, N., M. G. Pandy, et al. (2004). "Variation of neck muscle strength along the human cervical spine." Stapp Car Crash J **48**: 397-417.

Panjabi, M. M., T. Miura, et al. (2001). "Development of a system for in vitro neck muscle force replication in whole cervical spine experiments." Spine **26**(20): 2214-9.

Pintar, F., A. Sances, Jr, et al. (1990). Biodynamics of the total human cadaveric cervical spine. 34th Stapp Car Crash Conference, Orlando, Florida, USA, Society of Automotive Engineers, Inc., Warrendale, Pennsylvania, USA.

Saari, A., E. Itshayek, et al. (2006). Spinal cord deformation during injury of the cervical spine in head-first impact. 2006 International IRCOBI Conference on the Biomechanics of Impact Madrid, Spain.

Torg, J. S., J. T. Guille, et al. (2002). "Injuries to the cervical spine in American football players." J Bone Joint Surg Am. **84-A**(1): 112-22.

Yoganandan, N., F. A. Pintar, et al. (1989). Epidemiology and injury biomechanics of motor vehicle related trauma to the human spine. Stapp Car Crash Conference, SAE.

APPENDIX A

Figure A: Schematic of specimens number 1220 (A.1), 1221 (A.2), 1222 (A.3), 1223 (A.4), and 1224 (A.5). The occiput is shown at the bottom of the image, T2 is shown at the top and the injuries are indicated. The T1/2 casting cup, pulleys for the follower loads, and aluminum plate are also shown at the top of each image and the occiput adapter plate and screws in the occiput are shown at the bottom. ALL: anterior longitudinal ligament, BIL: bilateral, FC: facet capsule, Fx: fracture, ISL: interspinous ligament, IVD: intervertebral disc, L: left, LF: ligamentum flavum, R: right.